BioMetals (2006) 19:269–282
DOI 10.1007/s10534-005-8418-8

Quantification of hydroxamate siderophores in soil solutions of podzolic soil profiles in Sweden

Sofia A. Essén[1], Dan Bylund[1], Sara J. M. Holmström[1], My Moberg[2] & Ulla S. Lundström[1,*]
[1]*Department of Natural Sciences, Mid Sweden University, SE-851 70 Sundsvall, Sweden;* [2]*Department of Analytical Chemistry, Uppsala University, P.O. Box 599, SE-751 24 Uppsala, Sweden *Author for correspondence (Tel: +46-60-148416; Fax: +46-60-148820; E-mail: ulla.lundstrom@miun.se)*

Received 20 January 2005; accepted 06 June 2005

Key words: chromatography, ferrichrome, mass spectrometry, siderophores, soil

Abstract

Concentrations up to 2 and 12 nM of the hydroxamate siderophores ferrichrome and ferricrocin, respectively, were identified in soil solutions of podzolic forest soils at four sites in both northern and southern Sweden. No ferrichrysin was detected. As with the dissolved organic carbon and low molecular mass organic acids, the highest concentrations of the siderophores were found in the upper layers i.e. the mor layer, the eluvial and upper illuvial horizons. At the southern sites, the concentrations of ferrichrome and ferricrocin were both of similar magnitude and did not differ between the two sites. In contrast, soil solutions at the two northern sites contained more ferricrocin than ferrichrome; the ferricrocin concentrations were also higher at the northern sites than at the southern sites. Analyses were performed by high performance liquid chromatography with a porous graphitic carbon column on which ferrichrome, ferricrocin and ferrichrysin were separated. Detection by electrospray ionization mass spectrometry (ESI-MS) combined with on-line sample pre-concentration, by means of column-switching, enabled detection limits of 0.1–0.2 nM for ferrichrome, ferrichrysin and ferricrocin. The structural identities of the siderophores were further verified by MS/MS fragmentation. Fragmentation of ferrichrome, ferricrocin and ferrichrysin occurred mainly via peptide cleavage. The most intense fragments were typified by the loss of one of the three iron(III) chelating hydroxamate residues, i.e N5-acyl-N5-hydroxy ornithine.

Introduction

Iron is one of the major elements in the earth crust but biological availability is still low under aerobic conditions due to formation of ferric oxides. In order to facilitate iron acquisition, bacteria, fungi and plants produce efficient iron(III) chelators commonly known as siderophores (Drechsel & Jung 1998). These compounds chelate iron(III) through various functional groups. The dominating chelating groups are hydroxamates, catecholates, and phenolates, but carboxylic, oxazoline, α-hydroxy carboxylate, and keto hydroxy bidentate siderophores have also been found. Additionally, hybrid siderophores with more than one type of ligand group exist (Neilands 1981; Winkelmann & Drechsel 1997). While bacterial siderophores are structurally diverse, fungal siderophores are dominated by hydroxamate siderophores (Drechsel & Jung 1998). Ferrichromes are trihydroxamate siderophores, usually based on a hexa-peptide structure. The ferrichrome analogues ferrichrome, ferricrocin and ferrichrysin, differ in the nature of two amino acids, where glycine in ferrichrome has been replaced by one serine in ferricrocin and two in ferrichrysin (Figure 1). Iron(III) is complexed by three N5-acyl-N5-hydroxy-ornithine residues and the iron(III) stability

constants are $10^{29.1}$, $10^{30.4}$ and $10^{30.0}$, for ferrichrome, ferricrocin and ferrichrysin, respectively (Crumbliss 1991).

Ferrichrome-type siderophores mainly chelate trivalent ions, i.e. iron(III), aluminium(III) and gallium(III). On the other hand, low molecular mass organic acids (LMMOAs) interact with cations in general. These acids are produced by decomposition of organic matter or are exuded by bacteria, fungi and plant roots. In contrast to the model trihydroxamate siderophore desferrioxamine B (DFOB), chelation of iron(III) by LMMOAs is strongly pH dependent at acidic and neutral pH (Cline *et al.* 1983; Kraemer 2004).

In soil, fungal weathering may increase nutrient bioavailability by physical and chemical processes (Hoffland *et al.* 2004). Excretion of both protons and ligands such as LMMOAs and siderophores may cause chemical weathering (Hoffland *et al.* 2004). Weathering rates of feldspar have been shown to increase in the presence of LMMOAs (Drever & Stillings 1997). Enhanced dissolution rates in the presence of 1–240 μM of the hydroxamate siderophore DFOB have been demonstrated for a number of minerals, among them the aluminosilicate mineral kaolinite (Rosenberg & Maurice 2003), hornblende (Liermann *et al.* 2000; Kalinowski *et al.* 2000), goethite (FeOOH) (Watteau & Berthelin 1994; Kraemer *et al.* 1999; Cheah *et al.* 2003), and for biotite and pyrite (Watteau & Berthelin 1994). Moreover, the iron(III) dissolution rate in the presence of DFOB was higher in comparison to the LMMOAs from

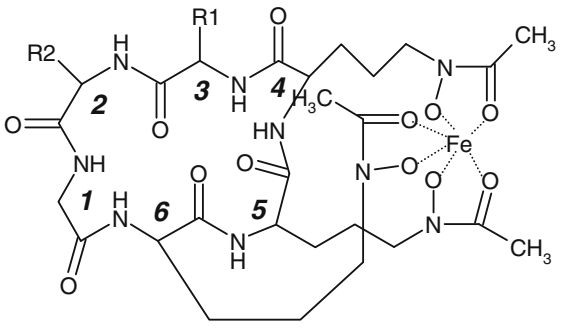

Figure 1. General structure of the studied ferrichromes, built up of six amino acids (No. 1–6). Ferrichrome, ferricrocin and ferrichrysin differs in amino acids 2 and 3. The amino acid sequences are gly-gly-gly-orn-orn-orn for ferrichrome (R2 = R1 = H), gly-ser-gly-orn-orn-orn (R2 = CH_2OH, R1 = H) for ferricrocin and gly-ser-ser-orn-orn-orn (R2 = R1 = CH_2OH) for ferrichrysin, where ornithine is N5-acyl-N5-hydroxylated.

both goethite (Watteau & Berthelin 1994) and kaolinite (Rosenberg & Maurice 2003). Weathering rates in mixtures of LMMOAs and DFOB have also been examined. In a mixture of 1–80 μM DFOB and 0–200 μM oxalate, Cheah *et al.* (2003) observed a synergistic effect on the increase of goethite dissolution. Kraemer (2004) suggests siderophores to enhance goethite dissolution by reducing the Gibbs free energy of the dissolution, therein facilitating dissolution by other ligands such as LMMOAs. In contrast, Watteau & Berthelin (1994) did not observe any synergism during dissolution of goethite by 125 μM DFOB and 80–2230 μM citric, oxalic and malic acids. Mor extracts have been shown to enhance dissolution rates of natural C-horizon soil and feldspars, i.e. microcline and labradorite (van Hees *et al.* 2002).

Soil solution and soil extracts have been shown to contain both LMMOAs and hydroxamate siderophores. Concentrations of total hydroxamate siderophores in the 27–279 nM DFOB equivalents range were found in soil extracts using the *Microbacterium flavescens* (former *Arthrobacter flavescens*) JG-9 assay (Powell *et al.* 1982), while Holmström *et al.* (2004) found approximately 1 nM ferrichrome in podzolic soil solution by an HPLC–MS method. Natural soil concentrations of LMMOAs are typically three orders of magnitude higher. In soil, concentrations of monocarboxylic acids *e.g.* formic, acetic and lactic acid are generally in the 0–1 mM range, whereas the content of di- and tricarboxylic aliphatic acids *e.g.* citric, oxalic and fumaric acids are typically in the 0–50 μM range with higher values in forested soils (van Hees *et al.* 1999, 2000; Strobel 2001). In Swedish podzols, values up to 400 μM of citric acid have been reported (van Hees *et al.* 1996, 1999, 2000).

Fungal production of siderophores may enhance plant uptake of mineral nutrients by symbiosis of ectomycorrhizal fungi and coniferous plants (Leyval & Berthelin 1989, 1991; Landeweert *et al.* 2001). Through cultivation of the fungi *Suillus granulatus* on goethite, Watteau & Berthelin (1994) noticed a decrease of pH and production of LMMOAs, mainly citric and malic acid, followed by a subsequent production of siderophores that promoted mobilisation of iron. Fungal production of ferrichrome-type siderophores has been demonstrated under pure culture conditions for a

number of ectomycorrhizal fungal species (Szaniszlo *et al.* 1981; Haselwandter & Winkelmann 2002), two ericoid mycorrhizal fungal species (Haselwandter *et al.* 1992), and two ectendomycorrhizal fungal species (Prabhu *et al.* 1996). Ectomycorrhizal fungi may produce more than one hydroxamate siderophore (Szaniszlo *et al.* 1981). Hoffland *et al.* (2004) suggest that fungal mineral weathering due to production of ligands such as LMMOAs is dominated by mycorrhizal fungi and lichens.

Quantification of hydroxamate siderophores has been accomplished by utilizing a variety of methods. These include determination of total iron ligand concentration by the CAS assay (Neilands & Nakamura 1991), determination of total amount of hydroxamate groups by the Czaky assay and growth stimulation of the bacterial strain *M. flavescens* (Powell *et al.* 1980). Similarly, the ferrichrome-type siderophores can be assayed by growth stimulation of *Escherichia coli* K-12 (Powell *et al.* 1983). None of these assays can be used for selective identification and quantification of specific siderophore compounds. Another drawback of using these techniques is the inability to analyse low concentrations, as the lowest detectable amount is in the range of 0.02 μmole for the Csaky assay and 0.002 μmole for the CAS assay (Neilands & Nakamura 1991).

Additionally, hydroxamate siderophores have been successfully separated by reversed phase high performance liquid chromatography, rp-HPLC (Jalal *et al.* 1984a; Konetschny-Rapp *et al.* 1988; Prabhu *et al.* 1996). Konetschny-Rapp *et al.* (1988) separated ferric complexes of 17 hydroxamate-type siderophores on C_8 and C_{18} HPLC columns using gradient elution and UV detection. However, the siderophores ferrichrome, ferricrocin and ferrichrysin do not separate satisfactorily using C_{18} columns (Jalal *et al.* 1984a; Konetschny-Rapp *et al.* 1988; Holmström *et al.* 2004). Furthermore, these HPLC methods have been used for analysis of pure cultures of mycorrhizal fungi, where siderophores have been enriched or samples have been concentrated by sample pre-treatment. Through UV detection, the detection limit was 1 μM, i.e., up to 1000 times higher than natural podzolic soil solution concentrations (Konteschny-Rapp *et al.* 1988). Combining chromatographic separation with selective mass spectrometry (MS) detection allows analysis and quantification of ferrichrome analogues in soil solution with a detection limit for ferrichrome of approximately 1 nM (Holmström *et al.* 2004), although ferrichrome and ferricrocin were not chromatographically separated. A method developed by Moberg *et al.* (2003), using on-line preconcentration by column-switching and separation on porous graphitic carbon column, enables separation of ferrichrome, ferricrocin and ferrichrysin with detection limits of 28–46 pM obtained by MS detection (Moberg *et al.* 2003). Via this switching technique, soil solution samples can be analysed without any prior pre-concentration or clean-up. Mass spectrometry also enables structural verification of siderophores by fragmentation (Gledhill 2001).

In this study, the concentration of ferrichrome, ferricrocin and ferrichrysin in soil solutions from podzolic soils at various depths at four sites in northern and southern Sweden were determined using HPLC–MS with on-line pre-concentration. The structures of ferrichrome and ferricrocin found in soil solution were verified by MS/MS fragmentation. Sampling occurred during the summer growth period, when the siderophore production is assumed to be at highest. The siderophore concentrations determined in this work were put in relation to previously reported data on soil solution chemistry (van Hees *et al.* 2000; Holmström *et al.* 2003) as well as to characterizations of the mycorrhizal communities (Rosling *et al.* 2003; Taylor & Finlay 2003) for the investigated sites.

Materials and methods

Chemicals

All water was purified by a MilliQ purification system (Millipore, Bedford, MA, USA) prior to use. Methanol and acetonitrile were of HPLC-grade (Chromasolv®), formic acid was of analytical grade and ammonium formiate was of p.a.-grade (all purchased from Sigma-Aldrich GmbH, Seelze, Germany). Iron-free ferrichrome, i.e. desferrichrome, was obtained from Sigma (St Loius, MO, USA) and desferricrocin and desferrichrysin were both purchased from EMC

Microcollections (Tübingen, Germany). Ferric siderophore complexes were prepared by addition of ferric chloride (p.a., Merck, Darmstadt, Germany)

Sampling sites

Samples were collected from podzolic soils at Hasslöv and Horröd in southern Sweden and at Heden and Nyänget in northern Sweden.

The Hasslöv area (56°24′ N, 13°00′ E) is forested with 50-year-old Norwegian spruce (*Picea abies*) on a Typic Haplorthod soil (Soil Taxonomy, Soil Survey Staff 1999). The horizons and their corresponding thickness are Olfh/Olf 6 cm, AE 9 cm and Bhs 37 cm. Samples were taken from three sample pits during the period June–July 1999. Hörröd is located 10 km SW of Hässleholm, Sweden (56 °05′ N, 13°39′ E) and is forested by about ~80-year-old Norwegian spruce (*Picea abies*). The soil is a well-drained homogenous Typic Haplorthod (Soil Taxonomy, Soil Survey Staff 1999) with the following soil horizon thickness: Oh/Of 7–10 cm, E/EA 6 cm (discontinuous) and Bhs/Bs approximately 40 cm with the top 10 cm as Bh. Samples were taken from three sample pits in early August 1998. A more detailed description of the chemistry, mineralogy and morphology of the Horröd and Hasslöv sites have been made by Bain *et al.* (2003).

Heden and Nyänget are both located in the Svartberget research park, 70 km NW of Umeå, Sweden (64°14′ N, 10°46′ E). In Nyänget, the tree layer consists of 60–80-year-old Norwegian spruce (*Picea abies*) and Scots pine (*Pinus sylvestris)* on a Typic Haplocryod soil (Soil Taxonomy, Soil Survey Staff 1998) developed on a till material with approximate horizon thickness O 10–15 cm, E 10–15 cm and B 40 cm. Samples were taken in early July 1996. The Heden site is forested with ~ 70-year-old Scots pine (*Pinus sylvestris)* and some Norwegian spruce (*Picea abies*) and Silver birch *(Betula pendula)*. The soil was an Entic Haplocryod (Soil Taxonomy, Soil Survey Staff 1998) based on fluvial sediment of 93% fine sand. The soil horizons in Heden were O 5 cm, E 5 cm and B 30 cm thick. Sampling took place in early July 1997. The Heden and Nyänget sites have been more thoroughly described by Ilvesniemi *et al.* (2000).

Sample preparation

Soil samples were collected by driving open-ended plastic cylinders (polyvinyl chloride, ID 4.6 cm, length 7 cm, volume about 120 ml) horizontally into the soil walls of a pit with length, width and depth of ~1 m. The plastic tubes containing soil cores were sealed with tight-fitting polyethylene lids. Eighteen replicate soil cores were taken from each pit and depth in Heden and Nyänget and 12–18 were taken in Horröd and Hasslöv. The organic mor layer soil was packed into plastic tubes after removal of green plant material. The soil samples were stored at 4 °C and soil water was extracted within 24 h after sampling by the soil drainage technique developed by Giesler & Lundström (1993). The soil cores were centrifuged for 30 min at 14000 rpm, i.e. 16500 g, using a Beckman J2-HS centrifuge equipped with a JA-14 rotor (Spinco division, Palo Alto, CA, USA). The soil water from the replicates was combined into one sample per pit and depth, which were then filtered (Millex-HV, 0.45 μm, Millipore, Bedford, MA, USA) and stored frozen to avoid degradation. Prior to analysis, the samples were again filtered (Millex-HV, 0.45 μm) to remove precipitation. Ferric iron was added to the samples before analysis to achieve complete ferric complex formation.

Quantitative analysis by capillary HPLC–MS

Quantification of the siderophores was performed via column-switching capillary HPLC–ESI–MS based upon the method developed by Moberg *et al.* (2003). The HPLC-system was built up of two microflow pumps (Perkin Elmer 200 Micro Series), both operated at 10 μl/min, and an auto-injector equipped with a thermostat (Agilent 1100, G1367A WPALS and G1330 ALSTherm, respectively). The injection volume was 70 μl and standards and samples were kept at 4 °C during analysis. The pre-column used for on-line concentration and purification was a Hypurity Aquastar C18 (30 × 0.50 mm, 5 μm, Thermo Hypersil-Keystone, Cheshire, UK) while the analytical column was a Hypercarb PGC (100 × 0.50 mm, 5 μm, Thermo Hypersil-Keystone, Cheshire, UK). Column-switching was obtained by a 10-port switch valve (VICI EPC10W, Valco Instruments, TX, USA). The total analysis time was 40 min. During the first

15 min, the pre-column was eluted to waste with mobile phase A (1% v/v methanol in ammonium formiate buffer, 11 mM, pH 4.0), following which it was backflushed towards the analytical column with mobile phase B (15% v/v acetonitrile in ammonium formiate buffer, 11 mM, pH 4.0). At 22 min, the pre-column was decoupled from the mobile phase B line and regenerated with mobile phase A. The ferric complexes of the analytes were detected by selected ion monitoring (SIM) of the proton adducts $[M + H]^+$, i.e. m/z 741.3 for ferrichrome, 771.3 for ferricrocin and 801.3 for ferrichrysin, on a triple quadrupole mass spectrometer (Sciex API 3000, Applied Biosystems, Canada) operated in positive electrospray ionization mode. By direct infusion at 10 µl/min (syringe pump Harvard Apparatus, Houston, MA, USA) the following MS parameter settings were found to give optimum sensitivity for the ions investigated: DP = 100 V, FP = 300 V and EP = 15 V.

A mixed stock solution containing 100 nM of each of ferrichrome, ferrichrysin and ferricrocin in formiate buffer (11 mM, pH 4.0) was prepared. The stock solution was further diluted to appropriate standard concentrations ranging from 0.02 to 20.0 nM of each of the three siderophores. The method was evaluated by determination of linearity, precision, limit of detection, system up-concentration factor (eq. 1), sample filtration recovery and sample matrix effects. Concentration limit of detection (C_{LOD}) and minimum detectable quantity (MDQ) are the injected concentration and amount of siderophore, respectively, that gives rise to a chromatographic peak height corresponding to three times the background noise. By assuming Gaussian peak shapes, the up-concentration factor (f) of the system was calculated for standard solutions by;

$$f = \frac{n_{inj}}{C_{inj} \times \upsilon \times w_{1/2}} \times \sqrt{\frac{5.54}{2\pi}} = \frac{V_{inj}}{\upsilon \times w_{1/2}} \times \sqrt{\frac{5.54}{2\pi}} \quad (1)$$

where C_{max} is the analyte concentration at chromatographic peak maximum, C_{inj} is the injected sample concentration, V_{inj} is the injection volume, υ is the volumetric mobile phase flow and $w_{1/2}$ the chromatographic peak width at half height.

The sample filtration procedure was tested by filtration of standard solutions of concentrations 2, 5, and 10 nM of each of ferrichrome, ferricrocin and ferrichrysin. Soil solution matrix effects were evaluated by sample spiking. One sample from the mor layer in Horröd plot 1 was spiked with 2, 5 and 10 nM of each siderophore, while 0.2 and 0.5 nM of each ferrichrome and ferrichrysin were added to samples from the illuvial horizon in Nyänget.

Structure identification by capillary HPLC-MS/MS

The previously described instrumental set-up was also used for HPLC–MS/MS analyses. The fragments were identified and the MS instrument tuned by direct infusion of 0.5 µM ferric ferrichrome analogue solution dissolved in mobile phase B at a flow rate of 5 µl/min, resulting in the following settings; DP = 100 V, FP = 300 V, EP = 10 V, CAD = 7, CE = 45 V and CXP = 15 V. Standard solutions and samples were prepared and chromatographically analysed according to the earlier description with the exception of a lowered injection volume of 50 µl. The identities of the monitored siderophores were verified for Nyänget samples from the mor layer and the upper and lower illuvial horizons by HPLC–ESI–MS/MS. Two fragments for each ferrichrome analogue were detected using multiple reaction monitoring (MRM), i.e. a common fragment of m/z 398 and neutral loss of 172 u corresponding to m/z 569 for ferrichrome, 599 for ferricrocin and 629 for ferrichrysin. The C_{LOD} for each detected fragment was determined as described for SIM detection.

Statistics

Statistical significance was established at 5% using Microsoft Excel 2000. The concentrations of ferricrocin and ferrichrome from Horröd and Hasslöv were compared via two-way analysis of variance (ANOVA). Comparison of the average concentration for each horizon between the northern and southern sites was then performed via t-test using the mean squared errors from the only above mentioned ANOVA as pooled estimates of the variances. Principal component analysis was performed using The Unscrambler®, v.7.5 (CAMO, ASA, Oslo, Norway). The model

contained soil solution pH, dissolved organic carbon (DOC, μM), total content of iron (μM), concentration (μM) of low molecular mass iron, i.e. complexes with molecular mass lower than 1000 Da, concentration (μM) of the LMMOAs formiate, acetate, propionate, lactate, oxalate, fumarate, malate, malonate, shikimate and citrate (data from van Hees *et al*. 2000; Holmström *et al*. 2003) and the siderophores ferrichrome and ferricrocin (nM) in mor layers, eluvial and illuvial horizons at Heden, Nyänget, Hasslöv and Horröd. All variables in the model were normalized to zero mean and unit variance.

Results

Quantification using capillary HPLC–MS

Evaluation of the analytical performance of the current method (Table 1) showed it to be linear in the concentration range up to 30 nM. The limit of detection was 0.21 nM for ferrichrome, 0.11 nM for ferricrocin and 0.06 nM for ferrichrysin. No soil solution matrix effects were found when one sample from the organic mor layer containing the highest concentrations of organic carbon such as LMMOAs was spiked with a mixture of ferrichrome analogues at concentrations typical of those found in soil solution. Additionally, no matrix effect was noted in the B-horizon sample for ferrichrysin, while the recovery of ferrichrome was 76–89% at a concentration corresponding to the detection limit.

The highest values found were 12 nM ferricrocin (Table 2) and 2 nM ferrichrome (Table 3) were found in soil solution from the sites, while ferrichrysin was not found in any of the analysed samples.

Significantly higher concentrations of ferricrocin were found in the mor layers at the sites in northern Sweden compared with the southern sites (*t*-test, $p < 0.05$). The distribution of ferricrocin along the soil profile also differed. At the southern sites, ferricrocin was most abundant in the eluvial and upper illuvial horizons, while the highest concentrations were found in the organic mor layer and the eluvial horizon at the northern sites (Table 2).

Similar levels of ferrichrome were found at the two southern sites as in Heden. Ferrichrome could not be quantified in the soil solution from Nyänget (Table 3). At all four sites, the highest quantites of ferrichrome were found in the upper layers, i.e. the mor layer and the eluvial horizon. At the southern sites, soil solution concentrations of ferrichrome and ferricrocin were similar. The ANOVA showed no significant interactions between sampling depth

Table 1. Evaluation of the HPLC–MS quantification method for the ferrichromes.

	Ferrichrome	Ferricrocin	Ferrichrysin
Linearity ≤ 30 nM			
Corr. coeff. ($n = 2 \times 8$)	> 0.999	> 0.999	> 0.999
Precision ($n = 6$)[a]			
0.5 nM	17%	19%	23%
5.0 nM	10%	11%	13%
Limit of detection			
C_{LOD}	0.213 nM	0.105 nM	0.058 nM
MDQ	1.1 fmole	0.52 fmole	0.29 fmole
Sample up-conc. factor			
(50–70 μl inj.)	5–10 times	8–12 times	11–14 times
Filtration recovery[b]	96–110%	98–106%	96–105%
Spiking recovery[c]			
Mor layer, 2, 5 and 10 nM	95–106%	94–104%	93–101%
Eluvial horizon, 0.2–0.5 nM	76–89%	–	105–111%

[a]Reported as relative standard deviation (%) of six injections.[b]Recovery of concentration in solution before filtration.[c]Recovery of added amount siderophore in spiked samples.

Table 2. Concentration of ferricrocin (nM) in soil solution from north (Heden and Nyänget) and south (Hasslöv and Horröd) of Sweden, quantified by on-line preconcentration column-switching HPLC–MS using SIM detection of the ferric $[M+H]^+$ ion at m/z 771.3.

Soil layer	Heden	Nyänget	Hasslöv			Horröd		
			Plot 1	Plot 2	Plot 3	Plot 1	Plot 2	Plot 3
Mor layer	12	4.4	0.42	0.12	1.82	0.43	0.84	0.60
Eluvial (E) horizon								
0–5 cm of E	2.9	2.8	2.3	0.23	3.3	1.0	5.9	4.4
5–10 cm of E	–	0.87	–	–	–	–	–	–
Illuvial (B) horizon								
0–5 cm of B	1.5	0.79	1.5	1.2	1.5	0.73	1.6	4.4
5–10 cm of B	0.12	0.27	–	–	–	–	–	–
10–15 cm of B	0.14	bdl	–	–	–	–	–	–
15–20 cm of B	–	–	0.14	0.49	0.17	0.28	0.19	0.45
Parent mat. (C)								
0–5 cm of C	bdl	0.15	–	–	–	–	–	–
40–45 cm of C	bdl	nd	–	–	–	–	–	–

For each soil layer, the depth was measured from the top of each horizon, *i.e.* the mor layer, the eluvial and illuvial horizons and the parent material. Mean value of triplicate injections. – = not analysed, nd = not detected and bdl = below detection limit.

and sampling site, indicating that the soil profile distributions of ferrichrome and ferricrocin are similar at the two southern sites. By principal component analysis, it was shown that the distribution of ferricrocin appears to correspond to the levels of dissolved organic carbon and citric, acetic and oxalic acid (Figure 2). No conclusions can be drawn for ferrichrome as so few observations were above the detection limit of ferrichrome. The PCA model explained 86% of the total variance by six principal components.

Structural verification by capillary HPLC–MS/MS

The fragments of the three ferrichrome analogues, identified by collision-induced dissociation MS/MS experiments on standard solutions, can be divided into two classes. The first class of fragments originates from loss of a similar residue from the three ferrichrome analogues, i.e. a loss of 18–229 amu (Table 4). The molecular masses of the three siderophores differ by 30 amu, corresponding to one $–CH_2OH$ unit. This is also the

Table 3. Soil solution concentration of ferrichrome (nM) detected as the ferric $[M+H]^+$ ion at m/z 741.3 (c.f. Table 2).

Soil layer	Heden	Nyänget	Hasslöv			Horröd		
			Plot 1	Plot 2	Plot 3	Plot 1	Plot 2	Plot 3
Mor layer	1.0	nd	1.4	nd	bdl	1.0	nd	1.5
Eluvial (E) horizon								
0–5 cm of E	0.61	nd	bdl	nd	0.42	2.1	bdl	2.0
5–10 cm of E	–	nd	–	–	–	–	–	–
Illuvial (B) horizon								
0–5 cm of B	bdl	bdl	bdl	bdl	bdl	0.81	bdl	0.46
5–10 cm of B	nd	bdl	–	–	–	–	–	–
10–15 cm of B	bdl	nd	–	–	–	–	–	–
15–20 cm of B	–	–	nd	bdl	nd	nd	bdl	nd
Parent mat. (C)								
0–5 cm of C	nd	nd	–	–	–	–	–	–
40–45 cm of C	nd	nd	–	–	–	–	–	–

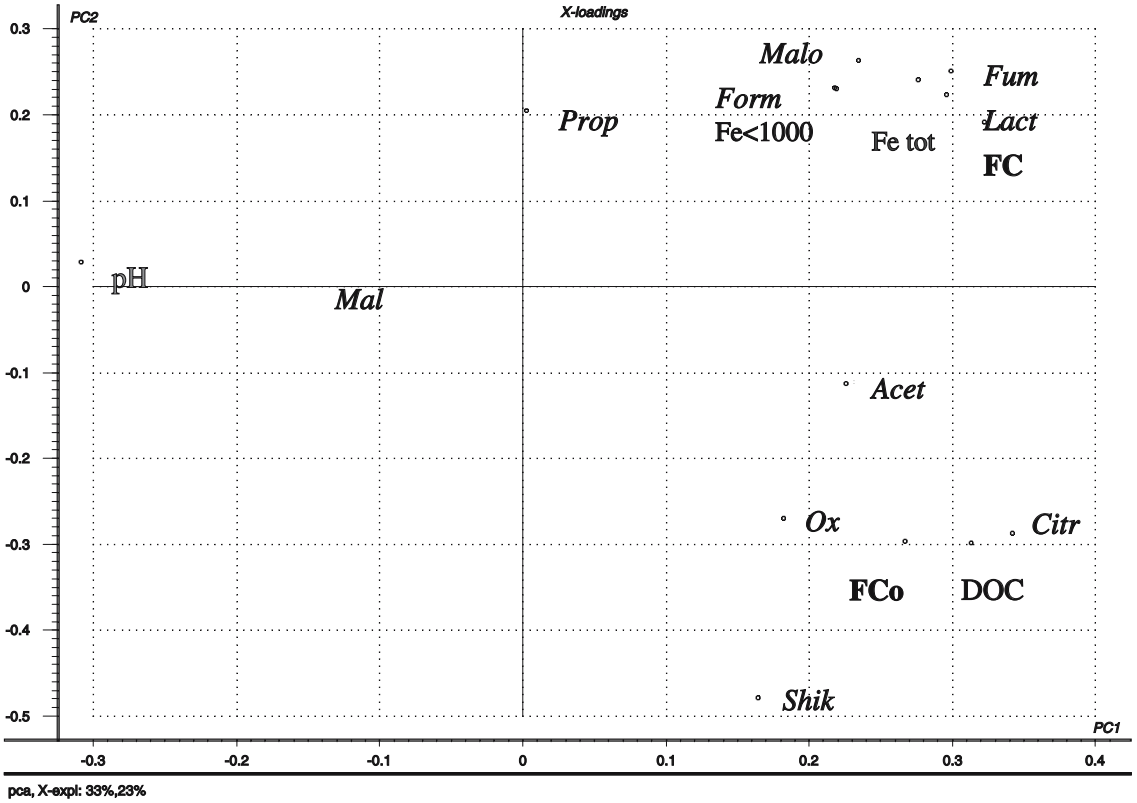

Figure 2. Loading plot of the two first principal components from principal component analysis (PCA) of soil solution pH (pH), concentration of dissolved organic carbon (DOC), concentration of organic acids: acetic (*Acet*), formic (*Form*), propionic (*Prop*), lactic (*Lact*), oxalic (*Ox*), citric (*Citr*), malonic (*Malon*), malic (*Mal*), fumaric (*Fum*) and shikimic (*Shik*) acids, total iron (Fe tot), low molecular mass bound iron (Fe < 1000), ferricrocin (**FCo**) and ferrichrome (**FC**). The two first components explained 33% and 23%, respectively of the total variance.

case for all fragments having lost the same residue. The second class of fragments has the same mass for all three ferrichromes (Table 5). These fragments originate from a part of the molecules that is identical for the three ferrichrome analogues. The fragments found were produced by loss of amino acids and by loss of water and CO (Table 4). The most intense fragments were produced by loss of

Table 4. Fragments of ferrichrome, ferricrocin and ferrichrysin that lost a similar neutral residue (neutral loss) in standard solution.

Ion	Loss (amu)	Ferrichrome		Ferricrocin		Ferrichrysin	
		m/*z* (amu)	Rel. int. (%)	*m*/*z* (amu)	Rel. int. (%)	*m*/*z* (amu)	Rel. int. (%)
$[M+H]^+$		741.5	100	771.4	100	801.4	100
$[M+H\text{-}H_2O]^+$	−18	723.4	6	753.5	32	783.5	37
$[M+H\text{-}CO]^+$	−28	713.5	15	743.5	13	773.4	18
$[M+H\text{-}2H_2O]^+$	−36					765.5	12
$[M+H\text{-orn}]^+$	−172	569.4	51	599.4	38	629.5	42
$[M+H\text{-orn}\text{–}H_2O]^+$	−190	551.5	2	581.3	11	611.4	10
$[M+H\text{-orn-}CO]^+$	−200	541.4	10	571.5	4	601.4	5
$[M+H\text{-orn-gly}]^+$	−229	512.4	9	542.4	10	572.4	2

The relative intensities are reported as peak height related to peak height of the most intense peak, *i.e.* the mother ion ($[M+H]^+$).
Abbreviations: M = ferric siderophore, gly = glycine, orn = N5-acyl-N5-hydroxy-ornithine, ser = serine.

Table 5. Fragments found for ferrichrome, ferricrocin and ferrichrysin with the same *m*/*z* for all three ferrichrome analogues in standard solutions.

Found fragment ion		Relative intensity (%)		
	m/*z* (amu)	Ferrichrome	Ferricrocin	Ferrichrysin
	599.4		38	4
[gly-ser-orn-orn-Fe]$^+$	542.4		10	17
[gly-orn-orn-Fe]$^+$	455.3	8	17	15
[orn-orn-Fe]$^+$	398.2	19	17	27

Relative intensity, collision energy and abbreviations as in Table 4.

one N5-acyl-N5-hydroxy-substituted ornithine (for simplicity called ornithine here) and a loss of ornithine-glycine (Table 4). The intensity of the fragment produced by loss of ornithine-glycine was higher for ferrichrome and ferricrocin in comparison to ferrichrysin. In contrast to ferrichrysin, both ferrichrome and ferricrocin have two ornithines connected to glycine. The intensity for the fragments corresponding to loss of water decreased in the series ferrichrysin > ferricrocin > ferrichrome. This trend corresponds to the number of $-CH_2OH$ groups, i.e. serine amino acids, in the molecule. For ferrichrysin, the loss of two water molecules was also observed.

The further loss of one amino acid – glycine or serine – from the fragment that already lost ornithine and glycine, resulted in identical fragment masses for ferrichrysin and ferricrocin of 542 amu (Table 5). Fragments at *m*/*z* 455, i.e. ferric glycine-ornithine-ornithine, and at *m*/*z* 398 composed of ferric ornithine-ornithine have the same masses for all three ferrichrome analogues. In this case, one compound specific fragment – the loss of one ornithine residue of 172 amu, and one common fragment, i.e. 398 amu – were chosen for verification of siderophore identities in soil solution.

The multiple reaction monitoring HPLC–MS/MS method was linear ($R^2 \geq 0.998$) between 0.05 and 5 nM for both fragments monitored for each ferrichrome analogue and can be used for quantification, although the limits of detection were slightly higher than for the HPLC–MS method (Table 6). The identities of ferrichrome and ferricrocin in the samples from Nyänget were confirmed by HPLC–MS/MS by detection of two fragments from the same mother ion as well as matching retention time (Figure 3).

Ferrichrome was found but could not be quantified by HPLC–MS/MS due to the higher detection limit. For ferricrocin, only the concentrations in the mor layer and the upper illuvial horizons (Table 6) were above the detection limit. Concentrations obtained by HPLC–MS/MS did not differ more than 10% from those found by HPLC–MS

Discussion

Selective analysis of ferrichromes, i.e. ferrrichrome and ferricrocin, in soil solution has only once been previously reported, in which 1 nM of ferrichrome was found in the mor layer and in the upper eluvial horizons of podzol soil solutions, some of which originate from the same sites as have been studied in this work (Holmström *et al*. 2004). Ferricrocin was also detected in some of the samples (Holmström *et al*. 2004). In this study, 0.1–12 nM ferricrocin was found in all podzol horizons, i.e. mor layer, eluvial, illuvial and C-horizon, with lower concentraions in the lower horizons, i.e. the illuvial horizon and the C-horizon. Similarily, most ferrichrome, i.e. up to 2.1 nM, was found in the mor layer and the eluvial horizon and decreased with depth below the detection limit. In contrast to this, no ferrichrysin was found in any of the samples in this study. The ferrichrome concentrations found in the mor layer and eluvial horizon here correlate well with the concentrations obtained by Holmström *et al*. (2004). Soil siderophore contents have earlier been estimatied as total hydroxamate siderophore as well as ferrichrome-type siderophore concentrations in extracts of dried soils using microbial assays (Powell *et al*. 1982, 1983). The total hydroxamate concentrations were in the 27–279 nM range,

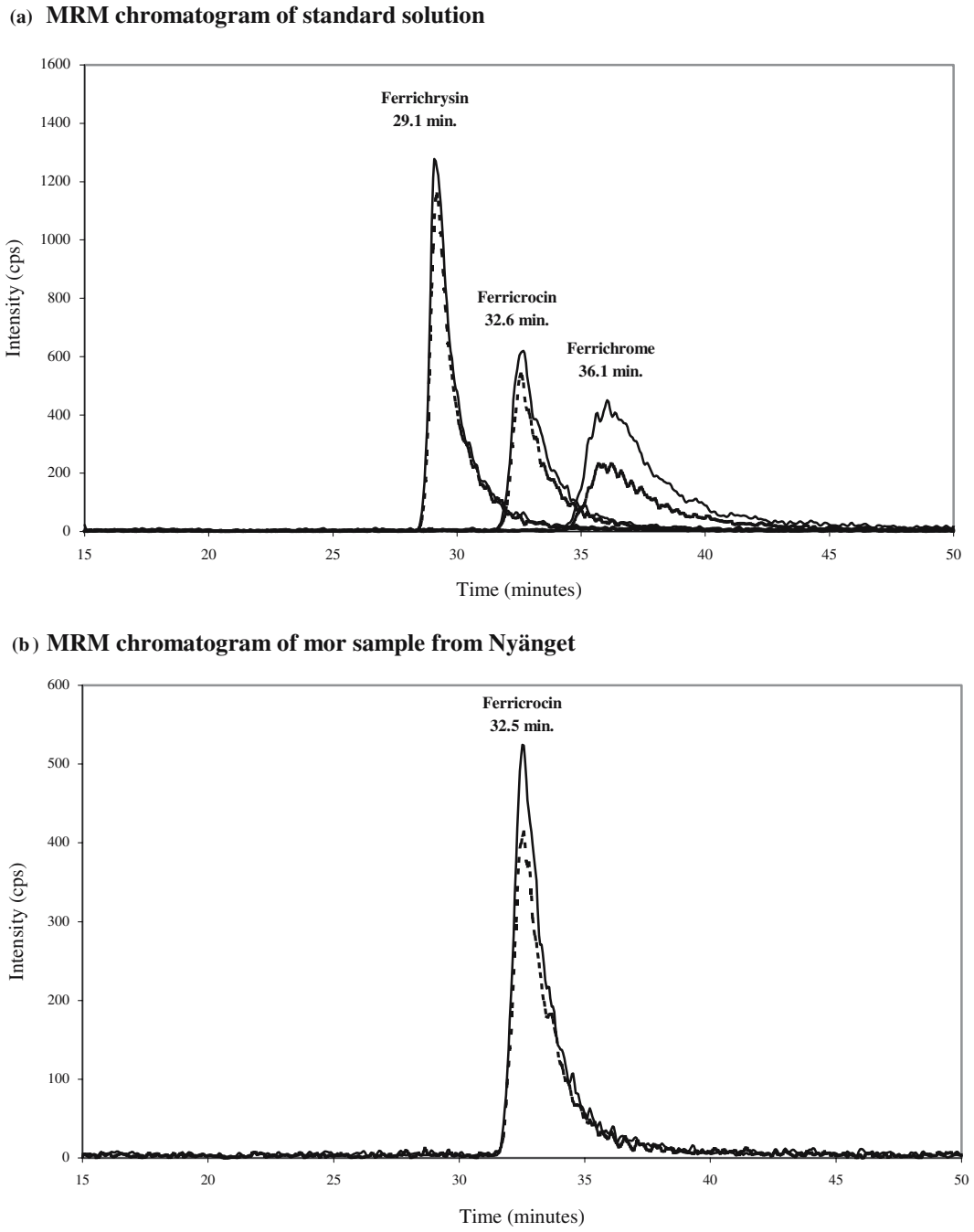

Figure 3. MRM chromatograms of (a) standard solution containing 5 nM ferric complexes of each of ferrichrysin, ferricrocin and ferrichrome and (b) a soil solution sample from the mor layer in Nyänget containing 3.9 nM ferricrocin. For each siderophore two fragments were detected, i.e. $[M+H]^+ \rightarrow$ 398 amu (- - - -) and a fragment corresponding to loss of one modified ornithine residue at 741 $\rightarrow$ 569 amu for ferrichrome, 771 $\rightarrow$ 599 amu for ferricrocin and 801 $\rightarrow$ 629 amu for ferrichrysin (– – –).

reported as DFOB equivalents and corrected to 10% soil moisture (Powell *et al.* 1982). In the extract of one soil, Powell *et al.* (1983) found 34 nM total hydroxamate siderophores by the *M. flavescens* assay. Remarkably, 78 nM of these were found to be of ferrichrome type by the *E. coli* assay

Table 6. Comparison of ferricrocin concentrations obtained by on-line preconcentration HPLC–MS (SIM) and HPLC–MS/MS (MRM) in samples from Nyänget.

Sample	SIM (nM)	MRM (nM)	
	m/z 771	m/z 771 → 398	m/z 771 → 599
Mor layer	4.36	3.91	3.88
Illuvial (B) horizon			
0–5 cm of B	0.79	0.71	0.70
5–10 cm of B	0.27	bdl	bdl
C_{LOD} (nM)	0.11	0.24	0.21

Sample layers, depths and number of injections as in Table 2.bdl, below detection limit.

(Powell *et al*. 1983). Thus, most of the hydroxamate siderophores in soils were suggested to be of ferrichrome type. However, the response of *M. flavescens* to different siderophores has been shown to vary (Jalal *et al*. 1984b), which makes interpretation of results from microbial assays difficult. Varying response on different siderophores may be one reason for the discrepancy of the *M. flavescens* and *E. coli* assay results reported by Powell *et al*. (1983). Despite non-selective analysis methods and variation in microbial response to different siderophores, the results by Powell *et al*. (1982, 1983) are of the same magnitude as the concentrations found in this work. By correction of the ferrichrome and ferricrocin concentrations to 10% soil moisture, as used by Powell *et al*. (1982, 1983), the corresponding concentrations found here were 1–79 nM ferricrocin and 0.9–6.7 nM ferrichrome in the upper horizons, i.e. the mor layer and the eluvial horizon at the two northern sites. Based on data obtained by microbial assays, approximated hydroxamate siderophore soil concentrations in the range 10–100 nM have been used for modelling mineral weathering (Kraemer 2004). In the present study, concentrations of up to 13 nM of two hydroxamate siderophores were measured and the approximations used by Kraemer (2004) seem reasonable as other hydroxamate siderophores, such as ferrioxamine, may additionally exist in soil (Moberg *et al*. 2004).

It is likely that both the identity and concentration of siderophores in soils are influenced by the ectomycorrhizal community. These communities have been investigated in the upper soil in Heden and Horröd (Taylor & Finlay, 2003), and throughout the soil profile in Nyänget (Rosling *et al*. 2003). Three years after the siderophore sampling in the vicinity of the Nyänget sampling pit, the ferricrocin-producing fungus *Wilcoxina rehmii* (Prabhu *et al*. 1996) was found in the C-horizon (Rosling *et al*. 2003), where ferricrocin was also found (Table 2). *Wilcoxina* forms ectendomycorrhiza with pine (*Pinus*) and ectomycorrhiza with spruce (*Picea*) (Smith & Read 1997). Characterization of ectomycorrhizal community and siderophores sampling was conducted in the same plots and at the same time in Horröd and Hasslöv. In Horröd, *Cenococcum geophilum* constituted 23% and 30% of the ectomycorrhizal community in sample plots 2 and 3, respectively, but was absent in sample plot 1. Ferricrocin has been identified as the main siderophore produced by *C. geophilum* under pure culture conditions (Haselwandter & Winkelmann 2002). The two plots where *C. geophilum* was found contained higher levels of ferricrocin in the mor layer and eluvial horizon than sample plot 1, where no *C. geophilum* was found. In addition, one species of *Boletus* was found in one of the plots in Horröd. Under pure culture conditions, *Boletus edulis* has been shown to produce several hydroxamate siderophores of which one was identified as ferricrocin by thin layer chromatography (Szaniszlo *et al*. 1981). The siderophore production of many ectomycorrhizal fungi is, however, still unknown. Fungi other than ectomycorrhizal species may also produce hydroxamate siderophores (Haselwandter 1995; Bartholdy *et al*. 2001).

The majority of the mycorrhiza-infected roots was found in the upper soil horizons (Rosling *et al*. 2003), where also the highest concentrations of ferrichrome and ferricrocin were detected. The highest quantities of DOC and LMMOAs were also found in the upper horizons (van Hees *et al*. 2000; Holmström *et al*. 2003). As illustrated by PCA modelling, the concentration of ferricrocin

showed a pattern similar to the concentration distributions of acetic, oxalic and citric acid (Figure 3). In this study, the highest total concentration of the studied ferrichrome-type siderophores was 13 nM, while the total concentration of LMMOAs ranged from 4–318 μM (van Hees *et al.* 2000; Holmström *et al.* 2003) in soil solution. In these concentration ranges, a synergistic enhancement of goethite dissolution rates by combination of a siderophore (DFOB) and other ligands, such as organic acids, has been shown both in a modelling experiment (Kraemer 2004) as well as in a laboratory study (Cheah *et al.* 2003).

The effects of siderophores on weathering and plant nutrition might depend on both bulk and local, i.e. rhizosphere, concentrations and adsorption to soil. Concentrations of hydroxamate siderophores in rhizosphere soil can be up to 50 times higher in comparison to bulk soil (Reid *et al.* 1984). Adsorbed siderophores may constitute a pool of bioavailable iron(III). In laboratory experiments, 83–100% of added DFOB adsorbed to soil (Powell *et al.* 1982). Both metal-free and cadmium-complexed DFOB has been shown to adsorb to humic substances (Higashi *et al.* 1998). Cline *et al.* (1983) found that adsorption of desferrichrome A was lower in comparison to DFOB. Although both are trihydroxamates, DFOB is positively charged at neutral pH due to a primary amine, while desferrichrome A has three carboxylic groups and is neutral or negatively charged depending on pH. The ferrichrome siderophores studied in this work are more similar to ferrichrome A than DFOB, regarding molecular structure and charge. Hence, it is not unlikely that they may adsorb to soil in a similar way as ferrichrome A. Powell *et al.* (1980) compared the extraction recovery of DFOB and natural hydroxamate siderophores by repeated soil extractions and found that the natural hydroxamate siderophores were more easily desorbed than DFOB, although less than 1/6 of the natural hydroxamate content was recovered during the first extraction. It is noteworthy that in the adsorption/desorption studies by Powell *et al.* (1980) and Cline *et al.* (1983), the soils were dried prior to extraction. In contrast, here the soil solution has been obtained directly from moist soil.

In this study, the presence of ferrichrome and ferricrocin at different depths in podzolic soil solution was verified. Two ferrichrome-type siderophores were determined selectively and also structurally verified by MS/MS. The major fragments obtained by MS/MS in this study were produced by peptide cleavage, i.e. loss of amino acids. Loss of water or CO was also observed. Peptides generally fragment by cleavage of C–N bonds, i.e. by loss of amino acids, which has also been observed previously for ferrichrome (Kaltashov *et al.* 1997; Gledhill 2001). Here, all fragments produced by peptide cleavage lost at least one N5-acyl-N5-hydroxy ornithine residue, i.e. one of the iron(III) chelating hydroxamate groups. In ferrichromes, iron(III) is chelated in a distorted octahedral structure by the three modified ornithines (van der Helm *et al.* 1987). The LC–MS/MS fragmentation pattern shows that two ornithine residues are enough to keep iron complexed in the gas phase; this was also noted by Kaltashov *et al.* (1997). In addition to structural identity verification, the possibility to use HPLC–MS/MS for quantification of ferrichrome, ferricrocin and ferrichrysin was demonstrated. However, due to lower sensitivity and higher detection limits by the HPLC–MS/MS method, quantification was preferably accomplished by HPLC–MS.

Conclusion

Ferricrocin and ferrichrome were quantified in soil solution from various depths of podzolic forest soils. Ferricrocin was found in all soil horizons at all sample sites studied. Similar to DOC and LMMOAs, the highest concentrations of ferricrocin and ferrichrome were found in the upper soil horizons, i.e. the mor layer, eluvial and illuvial horizons. The siderophore concentrations found were in the low nanomolar range, but might be of biological significance for weathering and mineral nutrient uptake. For detection of low concentrations of siderophores in soil solution without prior sample pre-treatment, the utilization of column-switching capillary HPLC–MS and structural identification by capillary HPLC–MS/MS were suitable.

Acknowledgements

The work was funded by the European Regional Development Fund and the Swedish Natural Science Research Council.

References

Bain DC, Tau Strand L, Gustafsson JP, Melkerud P-A, Fraser AR. 2003 Chemistry, mineralogy and morphology of spodosols at two Swedish sites used to assess methods of counteracting acidification. *Water Air Soil Pollut Focus* **3**, 29–47.

Bartholdy BA, Berreck M, Haselwandter K. 2001 Hydroxamate siderophore synthesis by *Phialocephala fortinii*, a typical dark septate fungal root endophyte. *BioMetals* **14**, 33–42.

Cheah S-F, Kraemer SM, Cervini-Silva J, Sposito G. 2003 Steady-state dissolution kinetics of goethite in the presence of desferrioxamine B and oxalate ligands: implications for the microbial acquisition of iron. *Chem Geol* **198**, 63–75.

Cline GR, Powell PE, Szaniszlo PJ, Reid CPP. 1983 Comparison of the abilities of hydroxamic and other natural organic acids to chelate iron and other ions in soil. *Soil Sci* **136**, 145–157.

Crumbliss AL. 1991 Aqueous solution equilibrium and kinetic studies of iron siderophore and model siderophore complexes. In: Winkelmann G (Ed.), *Handbook of Microbial Iron Chelates*. CRC Press Inc; Boca Raton: pp. 189

Drechsel H, Jung G. 1998 Peptide siderophores. *J Peptide Sci* **4**, 147–181.

Drever JI, Stillings LL. 1997 The role of organic acids in mineral weathering. *Coll Surfaces* **120**, 167–181.

Giesler R, Lundström U. 1993 Soil solution chemistry: Effects of bulking soil samples. *Soil Sci Soc Am J* **57**, 1283–1288.

Gledhill M. 2001 Electrospray ionisation-mass spectrometry of hydroxamate siderophores. *Analyst* **126**, 1359–1362.

Haselwandter K, Dobernigg B, Beck W, Jung G, Cansier A, Winkelmann G. 1992 Isolation and identification of hydroxamate siderophores of ericoid mycorrhizal fungi. *BioMetals* **5**, 51–56.

Haselwandter K. 1995 Mycorrhizal Fungi: Siderophore production. *Crit Rev Biotechnol*. **15**, 287–291.

Haselwandter K, Winkelmann G. 2002 Ferricrocin – an ectomycorrhizal siderophore of *Cenococcum geophilum*. *BioMetals* **15**, 73–77.

van der Helm D, Jalal MAF, Hossain MB. 1987 The crystal structures, conformations, and configurations of siderophores. In: Winkelmann G, Helm Dvan der, Neilands JB, eds. *Iron Transport in Microbes, Plants and Animals*. VCH; Weinheim: pp. 155–162.

van Hees PAW, Andersson A-MT, Lundström US. 1996 Separation of organic low molecular weight aluminium complexes in soil solution by liquid chromatography. *Chemosphere* **33**, 1951–1966.

van Hees PAW, Dahlén J, Lundström US, Borén H, Allard B. 1999 Determination of low molecular weight organic acids in soil solution by HPLC. *Talanta* **48**, 173–179.

van Hees PAW, Lundström US, Giesler R. 2000 Low molecular weight organic acids and their Al-complexes in soil solution-composition, distribution and seasonal variation in three podzolized soils. *Geoderma* **94**, 173–200.

Hees PAWvan, Lundström US, Mörth C-M. 2002 Dissolution of microcline and labradorite in a forest O horizon extract: the effect of naturally occurring organic acids. *Chem Geol* **189**, 199–211.

Higashi RM, Fan TW-M, Lane AN. 1998 Association of desferrioxamine with humic substances and their interaction with cadmium(II) as studied by pyrolysis–gas chromatography–mass spectrometry and nuclear magnetic resonance spectroscopy. *Analyst* **123**, 911–918.

Hoffland E, Kuyper TW, Wallander H, *et al*. 2004 The role of fungi in weathering. *Front Ecol Environ* **2**, 258–264.

Holmström SJM, Riise G, Tau Strand L, *et al*. 2003 Effects of lime and ash treatments on DOC fractions and low molecular weight organic acids in soil solutions of acidified podzol soils. *Water Air Soil Pollut Focus* **3**, 97–120.

Holmström SJM, Lundström US, Finlay RD, Hees PAWvan. 2004 Siderophores in forest soil solution. *Biogeochemistry* **71**, 247–258.

Ilvesniemi H, Giesler R, van Hees P, Magnusson T, Melkerud PA. 2000 General description of the sampling techniques and the sites investigated in the Fennoscandinavian podzolization project. *Geoderma* **94**, 109–123.

Jalal MAF, Mocharla R, van der Helm D. 1984a Separation of ferrichromes and other hydroxamate siderophores of fungal origin by reversed-phase chromatography. *J Chromatogr* **301**, 247–252.

Jalal MAF, Mocharla R, Barnes CL, *et al*. 1984b Extracellular siderophores from Aspergillus ochraceous. *J Bacteriol* **158**, 683–688.

Kalinowski BE, Liermann LJ, Givens S, Brantley SL. 2000 Rates of bacteria-promoted solubilization of Fe from minerals: a review of problems and approaches. *Chem Geol* **169**, 357–370.

Kaltashov IA, Cotter RJ, Feinstone WH, Ketner GW, Woods AS. 1997 Ferrichrome: Surprising stability of a cyclic peptide-Fe^{III} complex revealed by mass spectrometry. *J Am Soc Mass Spectrom* **8**, 1070–1077.

Konetschny-Rapp S, Huschka H-G, Winkelmann G, Jung G. 1988 High-performance liquid chromatography of siderophores from fungi. *Biol Met* **1**, 9–17.

Kraemer SM, Cheah S-F, Zapf R, Xu J, Raymond KN, Sposito G. 1999 Effect of hydroxamate siderophores on Fe release and Pb(II) adsorption by goethite. *Geochim Cosmochim Acta* **63**, 3003–3008.

Kraemer SM. 2004 Iron oxide dissolution and solubility in the presence of siderophores. *Aquat Sci* **66**, 3–18.

Landeweert R, Hoffland E, Finlay RD, Kuyper TW, Breemen Nvan. 2001 Linking plants to rocks: ectomycorrhizal fungi mobilize nutrients from minerals. *Trends Ecol Evol* **16**, 248–254.

Leyval C, Berthelin J. 1989 Interactions between *Laccaria laccata*, Agrobacterium radiobacter and beech roots: Influence on P, K, Mg and Fe mobilization from minerals and plant growth. *Plant Soil* **117**, 103–110.

Leyval C, Berthelin J. 1991 Weathering of a mica by roots and rhizospheric microorganisms of Pine. *Soil Sci Soc Am J* **55**, 1009–1016.

Liermann LJ, Kalinowski BE, Brantley SL, Ferry JG. 2000 Role of bacterial siderophores in dissolution of hornblende. *Geochim. Cosmochim. Acta* **64**, 587–602.

Moberg M, Holmström SJM, Lundström US, Markides KE. 2003 Novel approach to the determination of structurally similar hydroxamate siderophores by column-switching capillary liquid chromatography coupled to mass spectrometry. *J Chromatogr A* **1020**, 91–97.

Moberg M, Nilsson EM, Holmström SJM, Lundström US, Pettersson J, Markides KE. 2004 Fingerprinting metal-containing biomolecules after reductive displacement of iron by gallium and subsequent column-switched LC-IC-PMS analysis applied on siderophores. *Anal Chem* **76**, 2618–2622.

Neilands JB. 1981 Microbial transport compounds (siderophores) as chelating agents. In: Martell, Andersson, Badman,

eds. *Development of Iron Chelators for Clinical Use*. Elsevier; New York: pp. 13–14.

Neilands JB, Nakamura K. 1991 Detection, determination, isolation, characterization and regulation of microbial iron chelates. In: Winkelmann G, eds. *Handbook of Microbial Iron Chelates*. CRC Press Inc; Boca Raton: pp. 2–6.

Powell PE, Cline GR, Reid CPP, Szaniszlo PJ. 1980 Occurrence of hydroxamate siderophore iron chelators in soils. *Nature* **287**, 833–834.

Powell PE, Szaniszlo PJ, Cline GR, Reid CPP. 1982 Hydroxamate siderophores in the iron nutrition of plants. *J. Plant Nutr* **5**, 653–673.

Powell PE, Szaniszlo PJ, Reid CPP. 1983 Confirmation of occurrence of hydroxamate siderophores in soil by a novel *Escherichia coli* bioassay. *App Environ Microbiol* **46**, 1080–1083.

Prabhu V, Biolchini PF, Boyer GL. 1996 Detection and identification of ferricrocin produced by ectendomycorrhizal fungi in the genus *Wilcoxina*. *BioMetals* **9**, 229–234.

Reid RK, Reid CPP, Powell PE, Szaniszlo PJ. 1984 Comparison of siderophore concentrations in aqueous extracts of rhizosphere and adjacent bulk soils. *Pedobiologia* **26**, 263–266.

Rosenberg DR, Maurice PA. 2003 Siderophore adsorption to and dissolution of kaolinite at pH 3 to 7 and 22 °C. *Geochim Cosmochim Acta* **67**, 223–229.

Rosling A, Landeweert R, Lindahl BD, *et al*. 2003 Vertical distribution of ectomycorrhizal fungal taxa in a podzol soil profile. *New Phytol* **159**, 775–783.

Soil Survey Staff 1998 *Keys to soil taxonomy*. United Stated Department of Agriculture/Natural Resources Conservation Service.

Soil Survey Staff 1999 Soil taxonomy, A basic system of soil classification for making and interpreting soil surveys. second edition. United Stated Department of Agriculture/Natural Resources Conservation Service, Agriculture Handbook number 436.

Smith SE, Read DJ. 1997 Mycorrhizal symbiosis. (2nd ed.). Academic Press: 2; San Diego.

Strobel BW. 2001 Influence of vegetation on low-molecular-weight carboxylic acids in soil solution – a review. *Geoderma* **99**, 169–198.

Szaniszlo PJ, Powell PE, Reid CPP, Cline GR. 1981 Production of hydroxamate siderophore iron chelators by ectomycorrhizal fungi. *Mycologia* **73**, 1158–1174.

Taylor AFS, Finlay RD. 2003 Effects of liming and ash application on below ground ectomycorrhizal community structure in two Norway spruce forests. *Water Air Soil Pollut. Focus* **3**, 63–76.

Watteau F, Berthelin J. 1994 Microbial dissolution of iron and aluminium from soil minerals: efficiency and specificity of hydroxamate siderophores compared to aliphatic acids. *Eur. J. Soil Biol.* **30**, 1–9.

Winkelmann G, Drechsel H. 1997 Microbial siderophores. In: Rehm H-J, Reed G, eds. *Biotechnology: A multi-volume comprehensive treatise, volume 7 Products of secondary metabolism*. VCH; Weinheim: pp. 201.